Atmospheric Effects on Winter SO_2 Pollution in Lanzhou China

Peter C. Chu*

Naval Ocean-Atmospheric Prediction Laboratory, Naval Postgraduate School, Monterey, California, USA

Yuchun Chen and Shihua Lu

Cold and Arid Regions Environmental and Engineering Research Institute, Chinese Academy of Sciences, Lanzhou, China

*Corresponding author: Tel: +1-831-656-3688; Fax: +1-831-656-3686; E-mail address: pcchu@nps.edu
URL: http//www.oc.nps.navy.mil/~chu

Abstract

Lanzhou is one of the most polluted cities in China. SO_2 concentration has evident seasonal variability. It is generally within the second-level criterion (< 0.15 mg m^{-3}) in spring, summer, and fall, but is much higher than the second-level criterion and sometimes reaches mid level pollution (API > 200) in winter. Meteorological conditions (low winds, stable stratification) are found to be important for the SO_2 pollution. Observational and modeling studies conducted in this study show a close connection between the static stability and the SO_2 pollution of Lanzhou China in winter. This study also shows the capability of coupled RAMS-HYPACT on air-quality prediction.

Key words: SO_2 concentration, RAMS-HYPACT, air pollution index, stable stratification, inversion

1. Introduction

Lanzhou is located at a narrow (2-8 km width), long (40-km), NW-SE oriented valley basin (elevation: approximately 1,500-m) with the Tibetan plateau in the west, Baita mountain (above 1,700-m elevation) in the north, and the Gaolan mountain (above 1,900-m elevation) in the south (Fig. 1a). The aspect ratio of the valley (depth versus width) is around 0.07. Lanzhou contains four districts (Fig. 1b): Chengguan, Qilihe, Xigu, and Anning. Chengguan (District-I), located in the eastern valley, is the metropolitan area including government, commerce, culture, and residence. Xigu (District-III), located in the western valley, is the large heavy industrial area. Qilihe (District-II), located in the middle valley, and Anning (District-IV), located in the north middle valley, are the mixed residential, small factories, and farming (vegetables) area.

Annual and daily mean air quality standards for urban areas generated by the State Environmental Protection Agency (SEPA) are used as the air quality criteria. In Lanzhou, the second level standard is taken for the commercial and residential regions and the third level standard is taken for the industrial regions. For SO_2 pollutant, the annual mean second-level and third-level criteria are (0.06, 0.10 mg m^{-3}). The daily mean second-level and third-level criteria are (0.15, 0.25 mg m^{-3}) (Table 1). As the SO_2 concentration is higher than the air-quality criterion, the local SEPA will give the air-pollution alert.

Lanzhou is an industrial city famous for petrol-chemistry, metallurgy, and mechanical manufacturing. Fig. 2 shows the spatial distribution of annual SO_2 emission rate per square kilometer (unit: 10^3 kg km^{-2} yr^{-1}) in 2000. Emission rate is large in District-I (commercial and residential) and District-3 (industrial) (indicated with 'H' in Fig. 2). The total SO_2 emission from Lanzhou is 4.43×10^7 kg with 2.15×10^7 kg from industrial sources [Jiang et al., 2001].

The special topographic features of Lanzhou metropolitan area block the air streams due to the large frictional forces and causes weak winds. In the winter, the occurrence of the calm winds is nearly 80%. In the evening (occasionally even in the daytime) low-level inversion exists to inhibit turbulent diffusion. Lanzhou is one of the most polluted cities in China (Fig. 1c). Shang et al. [2001] show significant correlation between static stability and SO_2 concentrations. An air-quality monitoring system has been established in Lanzhou with multiple sampling and sufficient numbers of stations. This is the part of the project entitled Air Pollution and Control in Lanzhou (APCL), supported jointly by Gansu Province and the Chinese Academy of Sciences and carried out from 1999 to 2001.

In this study, the SO_2 pollution in Lanzhou metropolitan area is analyzed. Coupled Regional Atmospheric Modeling System (RAMS) and Hybrid Particle and Concentration Transport Model (HYPACT) [Tripoli and Cotton, 1982; Pielke Sr., et. al., 1992] are used to simulate diffusion and transport of SO_2. The objectives are to detect temporal and spatial SO_2 variability, to evaluate the air-quality objectively and

quantitatively, to analyze the pollutant sources, and to identify the effects of meteorology on the gaseous pollutant dispersion.

2. SO_2 Concentration

SO_2 monitoring system has been established in Lanzhou with multiple sampling and sufficient numbers of stations. This is the part of APCL, supported jointly by Gansu Province and the Chinese Academy of Sciences and carried out from 1999 to 2001. From the APCL project, the air quality data were collected at observational stations (St-1 - St-5) from October 1999 to April 2001 and at observational stations (St-6 - St-8) from August 2000 to April 2001. Over these stations, daily SO_2 concentration is calculated. Table 2 shows the geography of the stations and the temporal averages of SO_2 concentration in 2000 (January – December for station-1 to station-5 and August – December for station-6 to station-8). Station-5 (Yuzhong), located in a clean countryside, is taken as the reference station, where the annual mean SO_2 concentrations is less than the first-level national air quality criteria (comparison between Table 2 and Table 1). The data from routine air-quality observations include daily SO_2 concentrations were collected continuously by the SEPA in Lanzhou from June 2000 to May 2001 (station-E in Fig. 1b). Annual mean SO_2 concentrations are collected and computed from surface meteorological stations.

Fig. 3 shows the temporal variation of daily mean SO_2 concentrations at four APCL stations (St-1, St-3, St-4, and St-7) to represent District-I, District-II, District-III, and District-IV, respectively. The horizontal dashed and solid lines are referred to as the

second and third level criteria for daily mean concentrations (Table 1). The SO_2 concentration of the four stations is lower than the second level criterion (0.15 mg m^{-3}) all the time from April to October (late spring, summer and autumn) except few occasions. However, the SO_2 concentration exceeds the second level standard from December to January (winter) almost all the time and is sometimes higher than the third level standard (0.25 mg m^{-3}). The high SO_2 concentration in the winter is due to household heating. The maximum daily mean SO_2 concentration is 0.52 mg m^{-3} in December 2000 at station-1 (District-I). Additionally, the annual mean SO_2 concentration for station-1 (Table 2) is 0.08 mg m^{-3}, which also exceeds the second level annual mean standard: 0.06 mg m^{-3}.

At station-4 (District-III), the daily mean SO_2 concentration of also exceeds the second-level criterion from November to April and the pollution lasts much longer than that of any other observational stations. Besides, concentrations sometimes exceed the third-level criterion, with maxima of 0.40, 0.46, 0.47 mg m^{-3} in December, 1999, November, 2000, January, 2001, and monthly means of 0.21, 0.22, 0.20 mg m^{-3} in November, 1999, December, 1999, November, 2000 respectively. Annual mean SO_2 concentration at station-4 (Table 2) is 0.08 mg m^{-3}, larger than the second-level criterion (0.06 mg m^{-3}). Similarly, the daily mean SO_2 concentration at station-3 (District-II) and station-7 (District-IV) often exceeds the second-level criterion in December and January.

3. Air Pollution Index

Air pollution index (API) is a quantitative measure for uniformly reporting the air quality for different constituents and connects to the human health. SEPA classifies the air quality standards into 5 major categories due to API values (Table 3): I (clean), II (good), III (low-level pollution), IV (mid-level pollution), and V (high-level pollution). The categories III and IV have two sub-categories: (III_1, III_2) and (IV_1, IV_2).

Daily mean API of SO_2 averaged over all the observational stations shows an evident seasonal variation with larger values (maximum around 200) in winter (low-level pollution, Category-III) and much smaller values (usually smaller than 100) in other seasons. Monthly mean API of SO_2 shows the similar seasonal variability with larger value in winter and much smaller value in other seasons. At the background station (St-5), API for SO_2 is less than 50 all the time (Fig. 4).

4. Numerical Modeling

Meteorological effects on winter SO_2 pollution in Lanzhou are simulated using the coupled RAMS-HYPACT model.

4.1. RAMS

Non-hydrostatic RAMS-4.3 [Pielke, et al., 1992] is used in this study. The horizontal grid uses a rotated polar-stereographic projection. The vertical structure of the grid uses terrain-following coordinate system. The top of the model domain is flat and the bottom follows the terrain [Tripoli and Cotton, 1982]. The standard Arakawa C grid is used. RAMS contains lots of physics processes such as turbulent mixing [Helfand and Labraga, 1988], long and short-wave radiation [Chen and Cotton, 1987], wet physics

describing the interaction among the cloud formation and the liquid, solid precipitation materials, the sensible and latent heat exchange between the atmosphere and multi-layer soil, surface vegetation and surface water, topographic dynamic affection and cumulus convection parameterization. In the numerical simulation, a flat bottom with elevation of 1460 m is assumed. This indicates that 850 hPa level is nearly at the land surface. See the RAMS website: **http://www.rams.atmos.colostate.edu** for more information.

4.2. HYPACT

HYPACT was developed to simulate the motion of atmospheric tracers such as surface deposition, evaporation and condensation, precipitation scavenging, and other complex physical and chemical interactions under the influence of winds and atmospheric turbulence [Walko et al., 2001]. It adopts mixed Lagrangian and Eulerian approaches [Hurley and Physick, 1993]. The Eulerian system in HYPACT is similar to RAMS: a scalar field is predicted with advection and diffusion. For small scale pollutant air mass during the initial state, the tiny-grid Lagrangian component represents sources with any size and maintenance of concentrated, narrow pollutant plumes until being broadened by atmospheric dispersion. The position of SO_2 plume is described by

$$X(t+\Delta t) = X(t) + (u+u')\Delta t$$
$$Y(t+\Delta t) = Y(t) + (v+v')\Delta t$$
$$Z(t+\Delta t) = Z(t) + (w+w')\Delta t$$

where (u, v, w) are the three-dimensional grid-scale wind components; and (u', v', w') are three-dimensional sub-grid scale (turbulence) wind components.

When the SO_2 plume becomes large enough to be recognized by the Eulerian system, the Eulerian method is used. The Lagrangian pollutant plume can be converted

into a concentration field and then advected using an Eulerian formulation. The location and concentration of SO_2 plume is predicted by HYPACT using meteorological output from the RAMS. While a purely Eulerian treatment for the calculation of SO_2 concentration using the RAMS is possible, the HYPACT module offers an alternative method for estimating atmospheric transport and dispersion that is not restricted by the spatial resolution of the RAMS model.

4.3. Boundary and Initial Conditions

At the surface, we use USGS vegetation 25-catogory with type-1 for urban/built-up land, and type-4 for mixed dry/irrigational plants (afforestation). The NCEP data along the lateral boundary (every 6 hours) of the largest box from December 1 to 31, 2000 are taken as the open boundary condition. One way nesting is used for the triple-nested grid system. The larger model provides the lateral boundary conditions for the smaller model using a 5 point-buffer zone. The NCEP reanalysis data on December 1, 2000 are taken as the initial condition. The atmosphere is at rest ($\mathbf{V} = 0$) with horizontally uniform temperature and specific humidity soundings, which are taken from NECP reanalyzed data for Lanzhou at 00 GMT [0700 Beijing time (BT)] on December 1, 2000. RAMS is integrated from the initial conditions with the temporally varying solar irradiance at the top of the atmosphere since December 1, 2000.

Using RAMS multiple grid nested scheme (Table 4), the model equations are solved simultaneously on any number of interacting computational meshes of differing spatial resolution. The time dependent model solution is first updated on the coarsest

grid. A tri-quadratic spatial interpolation is then performed to obtain values that are assigned to the spatial boundaries of a finer grid nested within a coarser grid. The model fields on the finer grid are then updated using the coarser grid interpolated values as the spatial boundary conditions. Once the finer grid is at the same time level as the coarser grid, local spatial averages of the fine grid fields are obtained and used to overlay the coarse grid fields. The two-way interaction between the nested grids is performed following the scheme by Clark and Hall [1991] and Walko et al. [1995].

Five nested grids and 25 vertical levels illustrated by Chu et al. [2005] are used. The vertical spacing is 200 m near the surface and increases to 800 m above 2400 m. The vertical grid structure is the same for all five nested grids. The outer grid (Grid-1) was a 40×30 grid with a horizontal resolution of 54 km and a time step of 90 s. The first nested grid (Grid-2) was a 38×29 grid with a horizontal resolution of 18 km and a time step of 30 s. The second nested grid (Grid-3) was a 38×29 grid with a horizontal resolution of 6 km and a time step of 10 s. The third nested grid (Grid-4) was a 38×29 grid with a horizontal resolution of 2 km and a time step of 10/3 s. The innermost grid (Grid-5) was a 62×42 grid with a horizontal resolution of 1 km and a time step of 5/3 s. The first three grid systems (grid-1 to grid-3) are centered at (103.8^{o}E, 36.06^{o}N). The last two grid systems (grid-4 to grid-5) are centered at (103.8^{o}E, 36.08^{o}N). Using this configuration enables the influence of relatively fine-scale topographic flows on ash dispersal and deposition to be assessed. After integrating RAMS model, the meteorological variables are inputted into HYPACT every hour.

4.4. SO_2 Pollution Sources

Pollution sources can be flexibly set in HYPACT as single or multiple, instantaneous, continuous, or time varying. The source geometry can be point, line, area, or volume with various orientations, based on the spatial dimensions and the shape of horizontal section of the actual pollution sources. Since only the total amount of SO_2 emission in 2000, $A(x, y)$, is available (see Fig. 2), the SO_2 emission rate is the temporal mean over the year.

4.5. Model Verification

The RAMS-HYPACT model predicted daily mean SO_2 concentration has been compared with the APCL data. Fig. 5 shows the observed daily mean with range (between maximum and minimum) and model predicted daily mean SO_2 concentration at the eight stations. The model predicted values are within the observational ranges in all the stations except St-1 (residential district), where the model predicted value (0.32 mg/m^3) is much smaller than the observed value (0.52 mg/m^3).

5. Atmospheric Effects

The atmospheric static stability has seasonal and diurnal variability. With weak winds, the atmosphere is statically stable in evening and unstable in daytime. If the diurnal variability is filtered out, the atmosphere is statically stable in winter and unstable in summer. The connection between static stability and SO_2 concentration should be similar for the diurnal and seasonal variability. Thus, we analyze the diurnal variations of static stability and SO_2 concentration simulated using the RAMS-HYPACT model to detect the effect of the atmospheric static stability. Fig. 6 shows temporally varying sounding averaged horizontally over the inner most grid area (Grid-5) predicted

by RAMS on December 12, 2002. Below 2000-m height, the lapse rate ($\gamma = -\partial T / \partial z$) during the evening is (0.025°C/100 m) on 0200 BT, (0.05°C/100 m) on 0600 BT, and near 0 on 2100 BT (Fig. 6). The sounding has evident inversion between 1700-m and 1850-m on 0600 BT, and between 1850-m and 2000-m on 2100 BT. The daytime (1700 BT, three hours after the local noon time) sounding (Fig. 6c) shows a linear lapse rate with the temperature decreasing from 2.2°C at 1550-m to -3°C at 2150-m ($\gamma = 0.87$°C/100 m). Since the dry-adiabatic lapse rate (Γ) is 0.98°C/100 m, the simulated lapse rate in the air column 500 to 600 m above the ground is always stable (day and night), i.e., $\gamma < \Gamma$. However, the static stability [proportional to $(\Gamma - \gamma)$] is strongest on 2100 BT and weakest on 1700 BT.

The model predicted sounding agrees with the observed sounding (Fig. 7) reasonably well. Below 2000-m height, the observed lapse rate in the evening is (0.18°C/100 m) on 0200 BT, near zero on 0600 BT and 2100 BT with evident inversions. The daytime (1700 BT) observed sounding (Fig. 7c) shows a linear lapse rate with the temperature decreasing from 3°C at 1550-m to -2°C at 2150-m ($\gamma = 0.83$°C/100 m). Thus, the observed lapse rate in the air column 500 to 600 m above the ground is always stable, i.e., $\gamma < \Gamma$. Similar to model results, the observed static stability is strongest on 2100 BT and weakest on 1700 BT.

The winter sounding shows two features: (1) stable stratification during day and night, and (2) strong stability at night and weak stability during the day. These features make SO_2 pollution very difficult to diffuse at night. After the accumulation during the

evening, the SO_2 concentration should reach maximum before dawn. Since the daytime the atmosphere becomes less stable, the SO_2 concentration should be minimum 2-3 hours after the local noon time. The model predicted spatial distribution of the SO_2 concentration along 36.12^{o}N (Fig. 8) has evident diurnal variation associated with the diurnal variation of the static stability: heavy SO_2 pollution at 0600 BT and light SO_2 pollution at 1700 BT.

6. Conclusions

(1) Special topographic features of Lanzhou metropolitan area (narrow and long valley) block the air streams due to the large frictional forces and causes weak winds. In the winter, the occurrence of the calm winds is nearly 80%. In the evening (occasionally even in the daytime) low-level inversion exists to inhibit turbulent diffusion and in turn to cause heavy SO_2 pollution.

(2) The SO_2 pollution largely depends on the emission source. Among the four districts, the SO_2 pollution is heavy in District-I (commercial and residential area) and District-III (heavy industrial area).

(3) SO_2 concentration has evident seasonal variability. It is generally within the second-level criterion (< 0.15 mg m^{-3}) in spring, summer, and fall, but is much higher than the second-level criterion and sometimes reaches mid level pollution (API > 200) in winter.

(4) The winter sounding in Lanzhou China has two features: (a) stable stratification during day and night, and (b) strong stability at night and weak stability during the day. It causes the SO_2 pollutants very difficult to diffuse at night. After the accumulation

during the evening, the SO_2 concentration reaches maximum before dawn. During the daytime the atmosphere is less stable, the SO_2 concentration reaches minimum 2-3 hours after the local noon time.

(5) Close connection between the static stability and the SO_2 pollution of Lanzhou China in winter is simulated using a coupled RAMS-HYPACT model. This work also shows the capability of the RAMS-HYPACT model in predicting air quality.

Acknowledgments

This work was jointly supported by the National Natural Science Foundation of China Major Programs No. 40305020, and the Naval Postgraduate School. The data for this study are provided by the program entitled "Air Pollution and Control in Lanzhou" jointly sponsored by the local government of Gansu Province and the Chinese Academy of Science.

References

Chen, C., and Cotton W.R., 1987. The physics of the marine stratocumulus-capped mixed layer. *Bound. Lay. Meteor.*, 25, 289-321.

Chu, P.C., S.H. Lu, and Y.C. Chen, 2005. A numerical modeling study on desert oasis self-supporting mechanism. Journal of Hydrology, 312, 256-276.

Clark, T.L., and W.D. Hall, 1991. Multi-domain simulations of the time dependent Navier-Stokes equations: Benchmark error analysis of some nesting procedures. J. Comput. Phys., 92, 456-481.

Helfand, H. M., and J. C. Labraga, 1988. Design of a non-singular level 2.5 second-order closure model for the prediction of atmospheric turbulence. J. Atmos. Sci*.,* 45**,** 113–132.

Hurley, P. J., and W. L. Physick, 1993. A skewed, homogeneous Lagrangian particle model for convective conditions. Atmos. Environ*.,* 27A**,** 619–624.

Jiang, J.H., Y.C. Chen, X.D. Peng, and F. Hu, 2001. Contributions of industrial and residential sources to atmospheric SO_2 concentration in winter over Lanzhou. Plateau Meteorol., 20 (suppl.), 15-21 (in Chinese with English abstract).

Pielke, R. A., W. R. Cotton, R. L. Walko, C. J. Tremback, W. A. Lyons, L. D. Grasso, M. E. Nicholls, M. D. Moran, D. A. Wesley, T. J. Lee and J. H. Copeland, 1992. A comprehensive Meteorological Modeling system –RAMS, Meteor. Atmos. Phys., 49, 69-91.

Shang K. Z., C. Y. Da, Y. Z. Fu, S. G. Wang, and D. B. Yang, 2001. Stable Energy in Lanzhou and its Effect on Air Pollution. Plateau Meteorol., 20 (1), 76-81 (in Chinese with English abstract).

Tripoli, G. J., and W. R. Cotton, 1982. The Colorado State University three-dimensional cloud/mesoscale model—1982. Part I: General theoretical framework and sensitivity experiments. J. Rech. Atmos., **16**, 185-219.

Walko, R.L., C.J. Tremback, R.A. Pielke, and W.R. Cotton, 1995. An interactive nesting algorithm for stretched grids and variable nesting ratios. J. Appl. Meteor., 34, 994-999.

Walko, R.L., Tremback, C.J., Bell, M.J., 2001. HYPACT Hybrid Particle and Concentration Transport Model, User's Guide. Mission Research Corporation, Fort Collins, CO.

Table Caption

Table 1. Air quality standards for annual and daily mean SO_2 concentrations (mg m^{-3}) used by the Chinese National Environmental Protection Agency.

Table 2. Location of observational stations and temporally total mean concentrations (mg m^{-3}) of SO_2 during the whole observational period. Note that the second-level annual mean criterion is 0.06 mg m^{-3} for SO_2.

Table 3. API and air quality management in China.

Table 4. Numerical features of the RAMS model.

Figure Caption

Figure 1: Lanzhou: (a) geography, (b) topography, and (c) LANDSAT-TM imagery representing air pollution on 3 January 2001.

Figure 2. Spatial distribution of annual SO_2 emission amount per square kilometer (unit: 10^3 kg km^{-2}) in 2000. Here, the industrial sources are indicated with underlines; high-level sources are represented by the enclosed solid curves marked as 'H'. The dashed contours are topography (unit: m).

Figure 3. Daily mean SO_2 concentrations (mg m^{-3}) at St-1, St-3, St-4 and St-7 representing four districts. Horizontal dashed line is daily mean second-level criterion, while horizontal solid line is daily mean third-level criterion. Note that the daily mean SO_2 concentration shows strong seasonal variability with heavier pollution in the winter than in the summer.

Figure 4. API over all the observational stations.

Figure 5. Simulated and Observed daily mean SO_2 Concentration (mg/m^3) on December 12, 2000.

Figure 6. Model simulated and horizontally averaged temperature profiles over the grid-5 region (i.e., Lanzhou) on December 12, 2000: (a) 0200 BT, (b) 0600 BT, (c) 1700 BT (three hours after the local noon time), and (d) 2100 BT.

Figure 7. Observed temperature profiles on December 12, 2000: (a) 0200 BT, (b) 0600 BT, (c) 1700 BT (three hours after the local noon time), and (d) 2100 BT.

Figure 8. Model simulated SO_2 concentration along 36.12^o N on December 12, 2000: (a) 0200 BT, (b) 0600 BT, (c) 1700 BT (three hours after the local noon time), and (d) 2100 BT.

Table 1. Air quality standards for annual and daily mean SO_2 concentrations (mg m^{-3}) used by the Chinese National Environmental Protection Agency.

Level of Criterion	Annual	Daily
1	0.02	0.05
2	0.06	0.15
3	0.10	0.25

Table 2. Location of observational stations and temporally total mean concentrations (mg m^{-3}) of SO_2 during the whole observational period. Note that the second-level annual mean criterion is 0.06 mg m^{-3} for SO_2.

Site	Longitude E	Latitude N	Height Above Surface (m)	Region	SO_2
St-1	103.84	36.04	25	Chengguan (District-1)	0.08
St-2	103.84	36.07	11	Chengguan (District-1)	0.03
St-3	103.71	36.08	15	Qilihe (District-3)	0.05
St-4	103.63	36.10	22	Xigu (District-2)	0.08
St-5	104.09	35.84	4	Yuzhong County	0.01
St-6	103.92	36.04	19	Chengguan (District-1)	0.02
St-7	103.74	36.10	15	Anning (District-4)	0.04
St-8	103.63	36.09	4	Xigu (District-2)	0.06

Table 3. API and air quality management in China.

Air Pollution Index	Air Quality Classification		Air Quality Description and Management
API ≤ 50	I	Clean	No action is needed.
50 < API ≤ 100	II	Good	No action is needed.
100 < API ≤150	III_1		Persons should be careful in outdoor activities.
		Low-level pollution	
150 < API ≤200			
	III_2		
200 < API≤ 250	IV_1		Persons with existing heart or respiratory illnesses are advised to reduce physical exertion and outdoor activities.
		Mid-level pollution	
250 < API≤ 300			
	IV_2		
API ≥300	V	High-level pollution	Air pollution is severe; The general public is advised to reduce physical exertion and outdoor activities.

Table 4. Numerical features of the RAMS model.

Nested Grid	Center Coordinate	Grid points	Grid Interval	Time Step
1st	103.8°E, 36.06°N	40×30	54 km	90 s
2nd	103.8°E, 36.06°N	38×29	18 km	30 s
3rd	103.8°E, 36.06°N	38×29	6 km	10 s
4th	103.8°E, 36.08°N	38×29	2 km	10/3 s
5th	103.8°E, 36.08°N	62×42	1 km	5/3 s

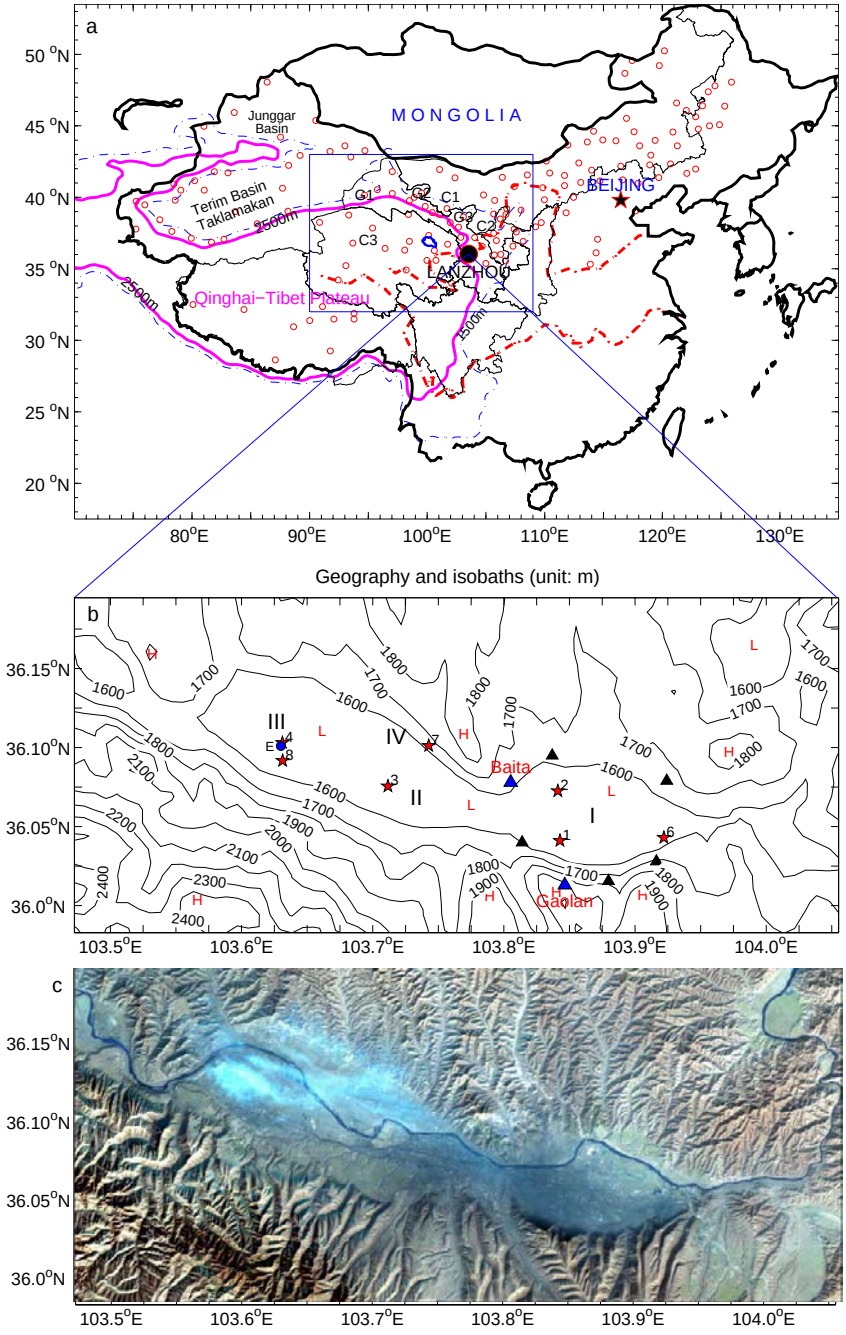

Figure 1: Lanzhou: (a) geography, (b) topography, and (c) LANDSAT-TM imagery representing air pollution on 3 January 2001.

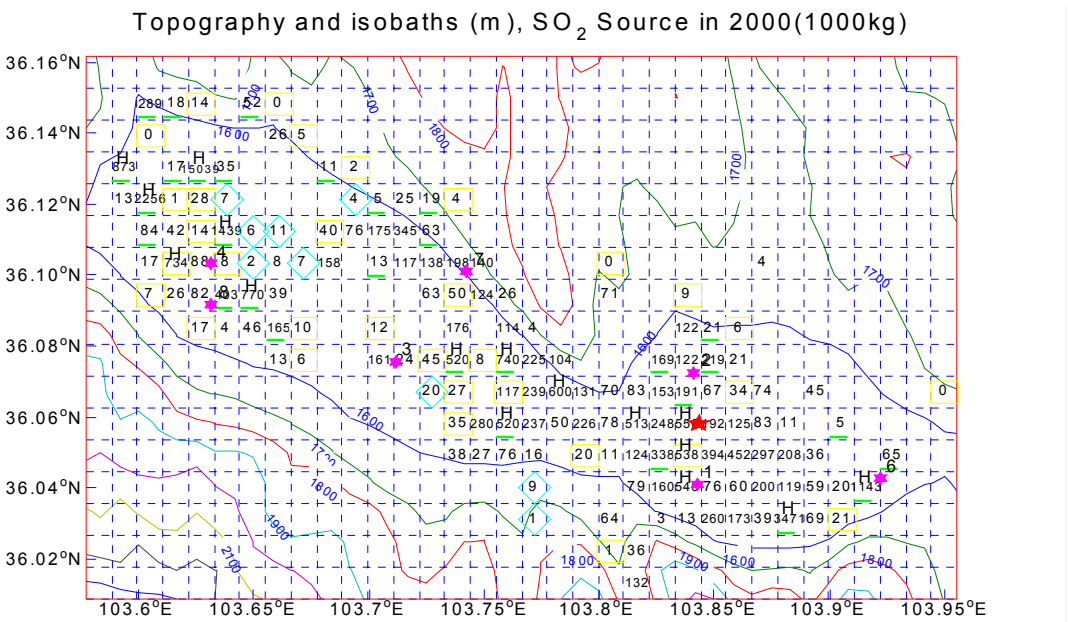

Figure 2. Spatial distribution of annual SO_2 emission amount per square kilometer (unit: 10^3 kg km^{-2}) in 2000. Here, the industrial sources are indicated with underlines; high-level sources are represented by the enclosed solid curves marked as 'H'. The dashed contours are topography (unit: m).

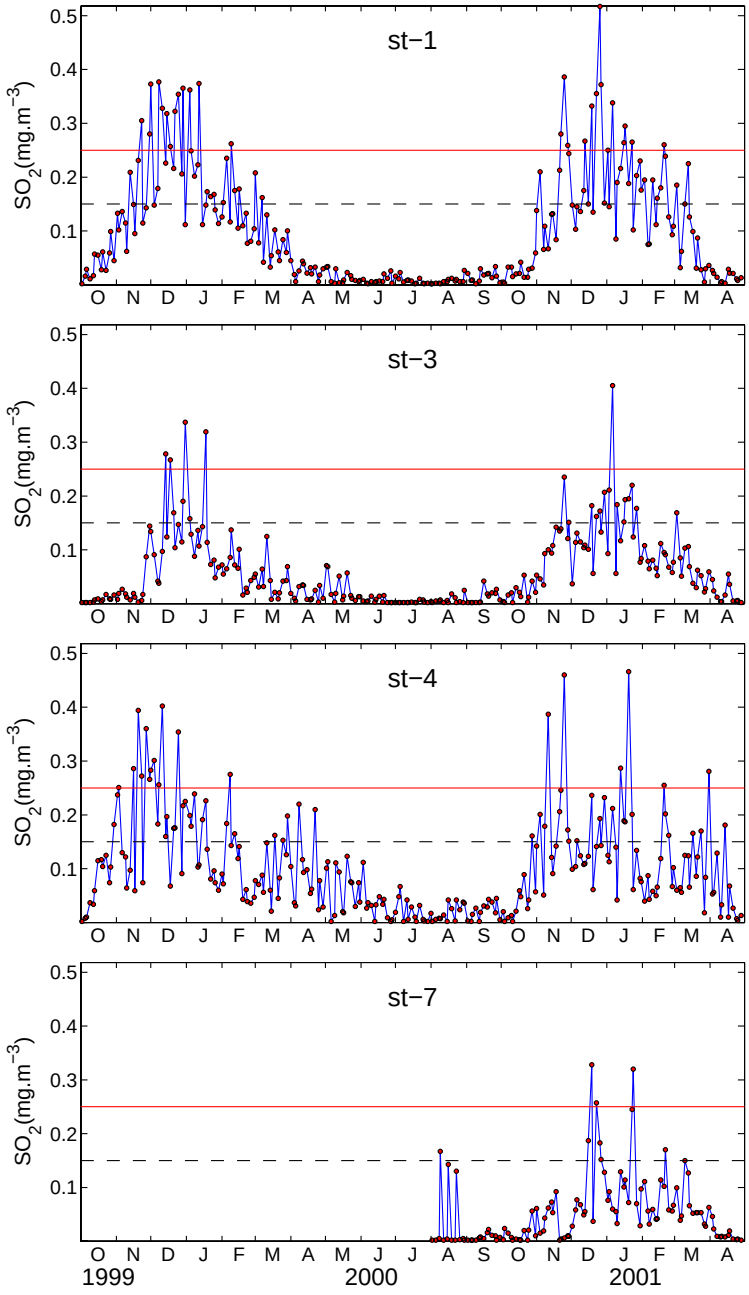

Figure 3. Daily mean SO_2 concentrations (mg m^{-3}) at St-1, St-3, St-4 and St-7 representing four districts. Horizontal dashed line is daily mean second-level criterion, while horizontal solid line is daily mean third-level criterion. Note that the daily mean SO_2 concentration shows strong seasonal variability with heavier pollution in the winter than in the summer.

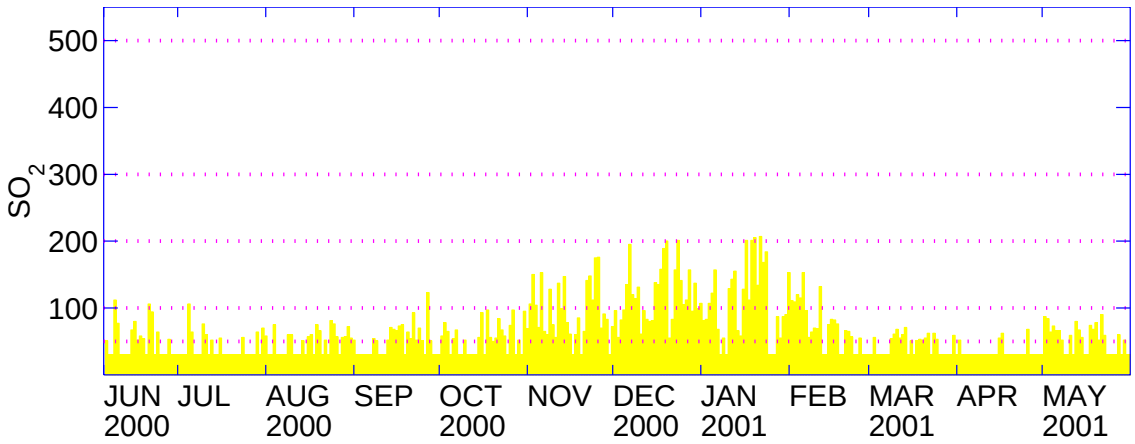

Figure 4. API over all the observational stations.

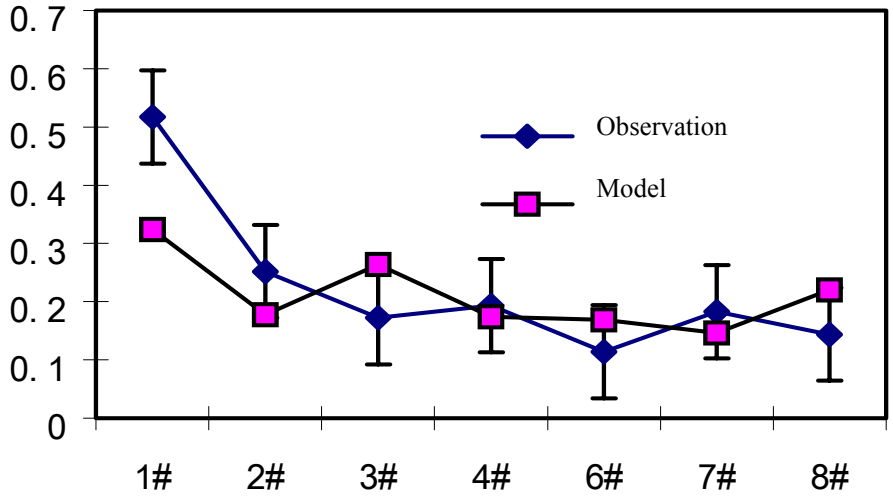

Figure 5. Simulated and Observed daily mean SO_2 Concentration (mg/m^3) on December 12, 2000.

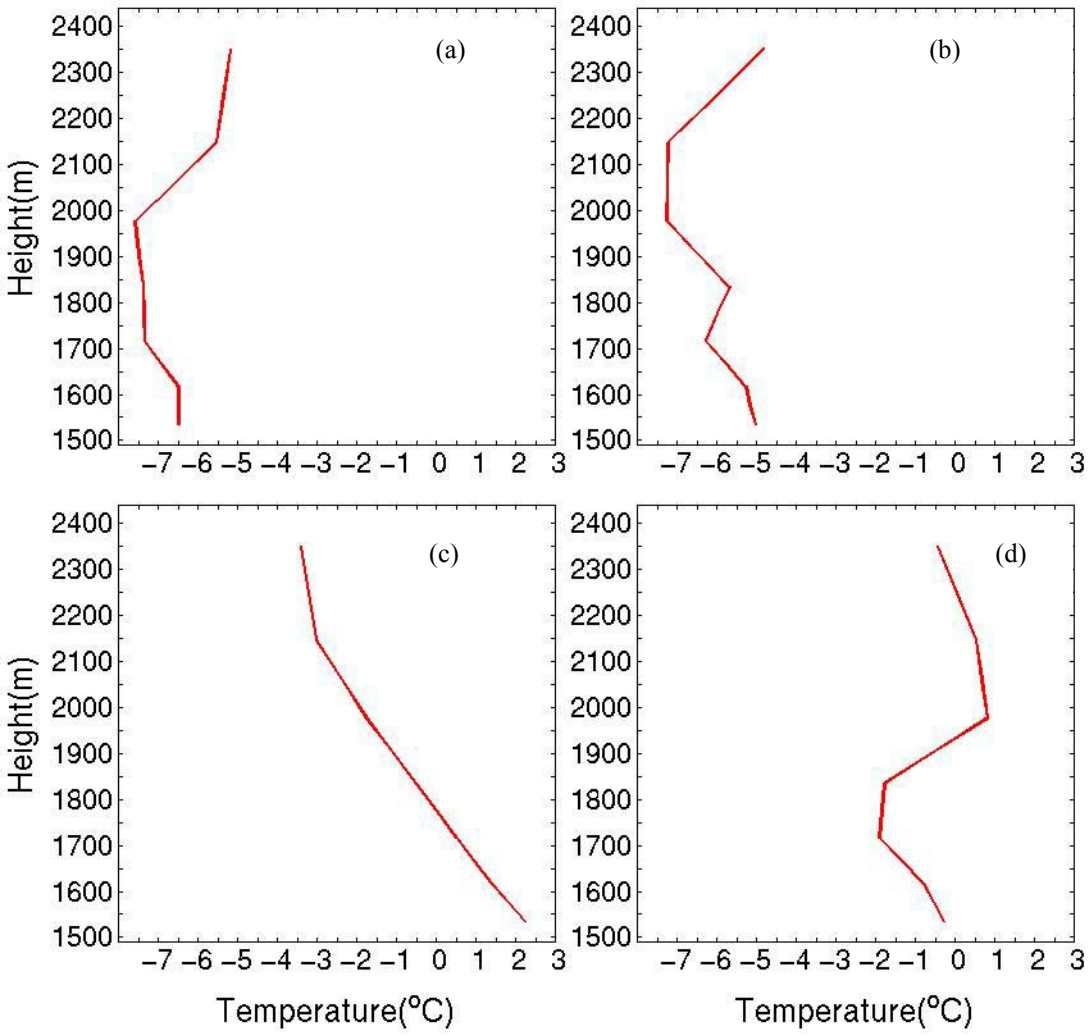

Figure 6. Model simulated and horizontally averaged temperature profiles over the grid-5 region (i.e., Lanzhou) on December 12, 2000: (a) 0200 BT, (b) 0600 BT, (c) 1700 BT (three hours after the local noon time), and (d) 2100 BT.

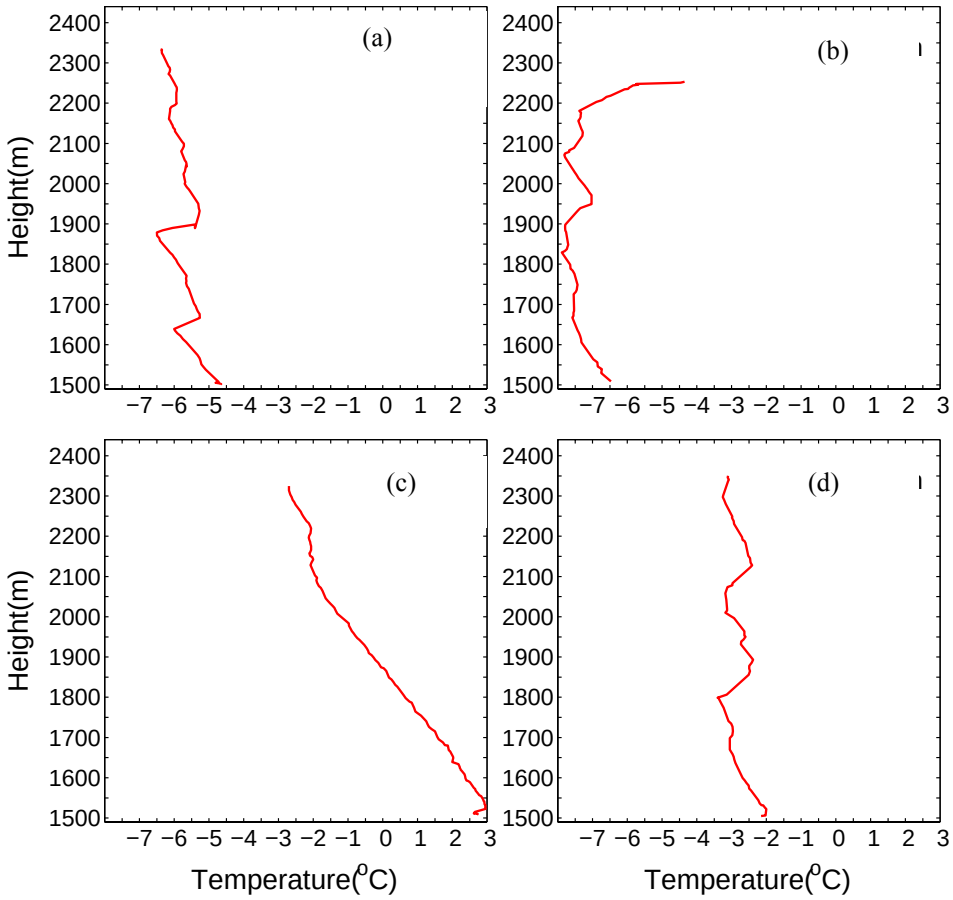

Figure 7. Observed temperature profiles on December 12, 2000: (a) 0200 BT, (b) 0600 BT, (c) 1700 BT (three hours after the local noon time), and (d) 2100 BT.

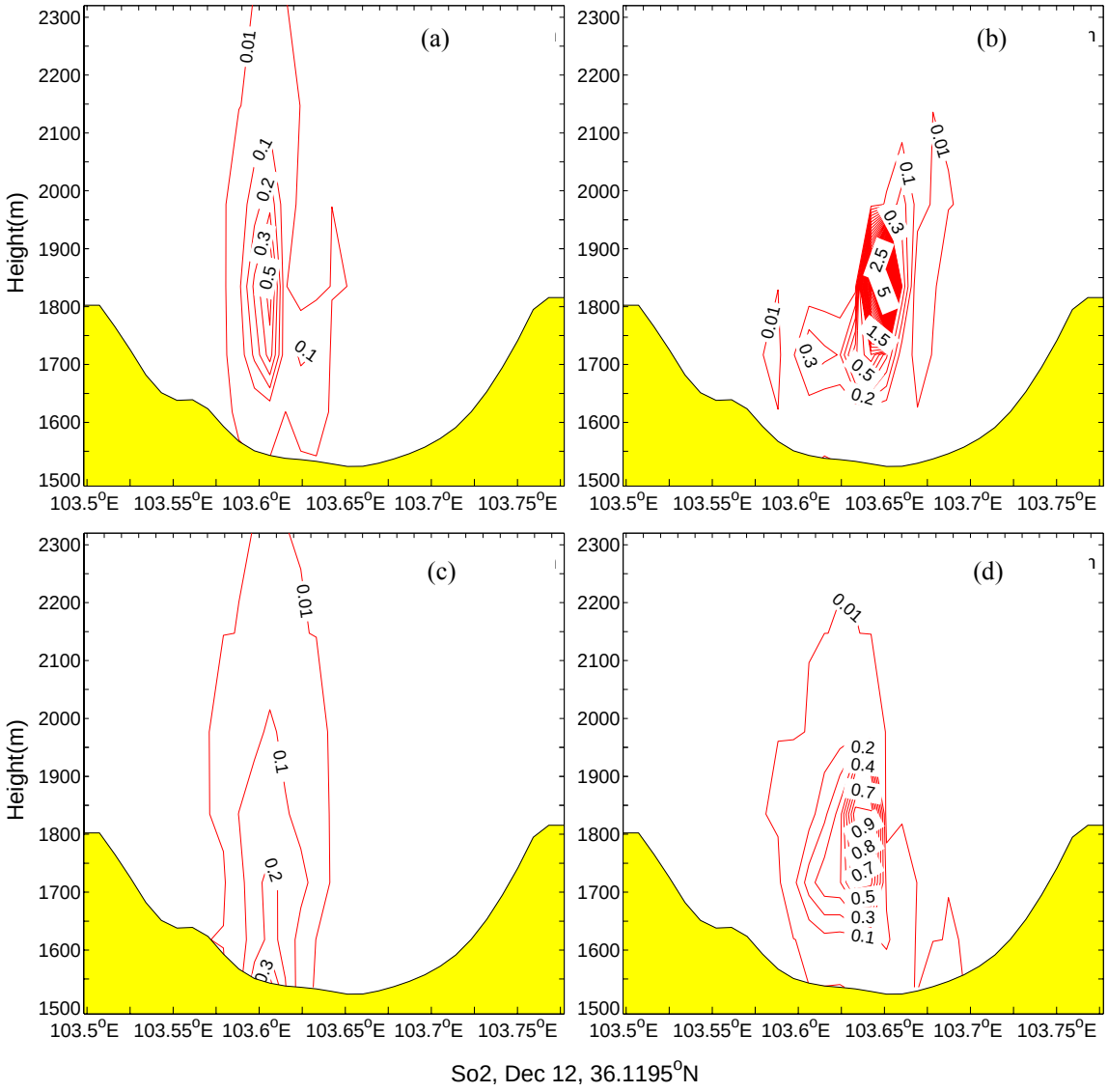

Figure 8. Model simulated SO_2 concentration along 36.12° N on December 12, 2000: (a) 0200 BT, (b) 0600 BT, (c) 1700 BT (three hours after the local noon time), and (d) 2100 BT.